

Comparison of Maximum Torque per Ampere and Loss Minimization Control for the Interior Permanent Magnet Synchronous Generator

Tin Bariša, Damir Sumina, Martina Kutija

University of Zagreb, Faculty of Electrical Engineering and Computing
Unska 3, 10000 Zagreb, Croatia

tin.barisa@fer.hr, damir.sumina@fer.hr, martina.kutija@fer.hr

Abstract— In this paper maximum torque per ampere and loss minimization control methods for an interior permanent magnet synchronous generator are compared. Permanent magnet synchronous generators have wide application in wind energy conversion systems due to high efficiency, high power density, high power factor and wide speed operating range. Maximum torque per ampere control method finds optimal d - and q -axis stator currents that produce desired electromagnetic torque while minimizing stator current magnitude. Loss minimization control method takes into account both copper and iron losses and finds optimal d - and q -axis stator currents that produce desired electromagnetic torque while minimizing total power loss. Characteristic curves for both control methods considering magnetic saturation are presented. Feed-forward torque control model developed in MATLAB/Simulink was used to verify described control methods.

Keywords— interior permanent magnet synchronous generator, maximum torque per ampere, loss minimization, torque control

I. INTRODUCTION

Permanent magnet synchronous generators (PMSG) have wide application in wind energy conversion systems (WECS) [1]-[3]. Main characteristics of a PMSG are high efficiency, high power density, high power factor and wide speed operating range. If PMSG is connected to grid by a full power back to back converter, the wind turbine can be operated to extract maximum wind power at different wind speeds by optimally adjusting shaft speed [4].

In case of interior permanent magnet synchronous generator (IPMSG) magnets are placed inside of rotor. As a result, inductance in the q -axis is bigger than inductance in the d -axis. This effect results in reluctance torque which depends on both the q - and the d -axis stator currents. If the d -axis stator current is equal to zero electromagnetic torque is proportional to the q -axis stator current [5]. However, in that case there is no reluctance torque and torque control of an IPMSG is not optimal. In order to produce reluctance torque several control algorithms have been developed such as constant flux linkage control [6], power unity control [6], maximum torque per ampere control [7]-[11], loss minimization control [12]-[16].

Maximum torque per ampere (MTPA) control method produces desired electromagnetic torque while minimizing current magnitude. In [7] MTPA control was applied in constant torque region while in constant power region flux weakening was used. In [8] lookup tables were used to achieve MTPA control considering magnetic flux variation caused by temperature. In [9] premade lookup tables are avoided by utilizing Ferrari's method to find solutions to quartic equations which represent optimal stator currents according to MTPA. In [10] Newton-Raphson iterative method was used to solve high-order nonlinear relationship between the electromagnetic torque reference, magnetic flux linkage and desirable dq -axis stator currents. In [11] normalized MTPA equations are presented and feed-forward torque control is proposed.

Loss minimization (LM) control method produces desired electromagnetic torque while minimizing total loss in an IPMSG. In [12] basic LM control algorithm which relies on mathematical model of an IPMSG including iron loss is established. In [13] an online adaptive loss minimization controller is presented which minimizes total input power by adjusting the d -axis stator current until the optimal point is reached. In [14] LM control is established using online binary search algorithm. In [15] LM control considering magnetic saturation and cross coupling is developed. For different electromagnetic torque references at given rotor speed, optimal stator currents are calculated and stored into a lookup table which is utilized in the torque control loop. In [16] lookup tables are avoided by utilizing analytic methods to solve quartic equations which represent optimal stator currents according to LM.

This paper is organized as follows. In Section II mathematical model of an IPMSG is given. Mathematical background for MTPA is provided and characteristic MTPA curve is presented. In Section III mathematical model of an IPMSG considering the iron loss is given. Mathematical background for LM is provided and characteristic LM curves for different rotor speed values are presented. In Section IV feed-forward torque control model for IPMSG in MATLAB/Simulink is used to verify MTPA and LM control methods. In Section V previously described control methods are compared and conclusion is given.

II. MAXIMUM TORQUE PER AMPERE

The mathematical model of an IPMSG in synchronously rotating dq reference frame can be expressed as follows:

$$u_d = R_s i_d + L_d \frac{di_d}{dt} - \omega_e L_q i_q \quad (1)$$

$$u_q = R_s i_q + L_q \frac{di_q}{dt} + \omega_e L_d i_d + \psi_m \omega_e \quad (2)$$

$$T_e = \frac{3}{2} p (\psi_m i_q + (L_d - L_q) i_d i_q) \quad (3)$$

where u_d and u_q are the d - and the q -axis stator voltages, i_d and i_q are the d - and the q -axis stator currents, ω_e is angular electrical speed, R_s is the stator resistance, L_d and L_q are the d - and the q -axis inductances, ψ_m is the permanent magnet flux linkage, T_e is the electromagnetic torque and p is the number of pole pairs. Since the effective air-gap length in the d -axis is large and relative magnetic permeability of permanent magnets is close to unity, inductance in the d -axis does not change significantly due to magnetic saturation. However, the effective air-gap length in the q -axis is small and therefore inductance in the q -axis changes significantly depending on the q -axis stator current [17]. Variations in the d - and the q -axis inductances of the IPMSG used in simulation are shown in Fig. 1.

Neglecting voltage drop on stator resistance, stator current and voltage limits are defined as follows:

$$i_d^2 + i_q^2 \leq I_{max}^2 \quad (4)$$

$$L_d^2 \left(i_d + \frac{\psi_m}{L_d} \right)^2 + L_q^2 i_q^2 \leq \frac{U_{max}^2}{\omega_e^2} \quad (5)$$

where I_{max} is maximum permissible current of drive and U_{max} is maximum available voltage. I_{max} depends on generator and power converter rated currents while U_{max} depends on modulation technique and DC-link voltage [10]. Current limit is in shape of a circle in dq plane while voltage limit forms ellipse which shrinks as generator speed increases as shown in Fig. 2.

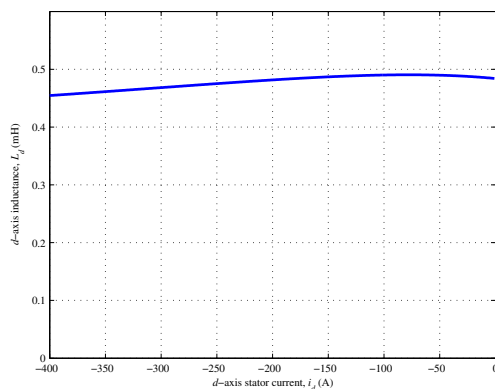


Fig. 1.a) d -axis inductance

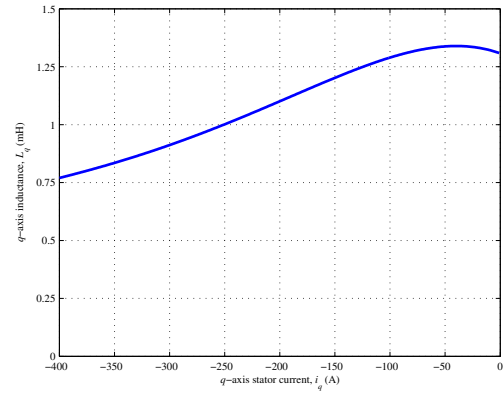


Fig. 1.b) q -axis inductance

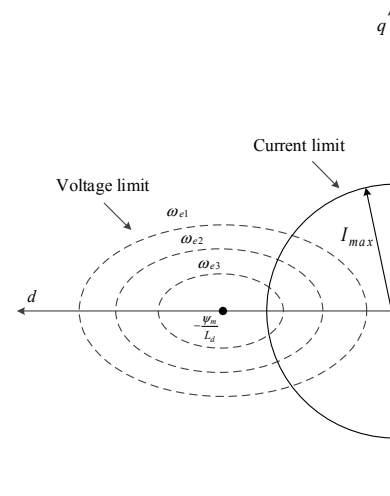


Fig. 2. Voltage and current limits

Vector diagram of an IPMSG is shown in Fig. 3. Stator currents in the d -axis and the q -axis can be expressed depending on the stator current angle as follows:

$$i_d = -I \sin \gamma \quad (6)$$

$$i_q = -I \cos \gamma \quad (7)$$

where γ is the stator current angle and I is the stator current magnitude. Using (6)-(7) the electromagnetic torque equation (3) can be written as follows:

$$T_e = \frac{3}{2} p \left(-\psi_m I \cos \gamma + \frac{1}{2} (L_d - L_q) I^2 \sin 2\gamma \right) \quad (8)$$

The electromagnetic torque expressed as (8) is a function of the stator current angle and the stator current magnitude. In order to find the maximum electromagnetic torque for given stator current magnitude (i.e. minimum stator current magnitude for given electromagnetic torque), $\partial T_e / \partial \gamma = 0$ is calculated.

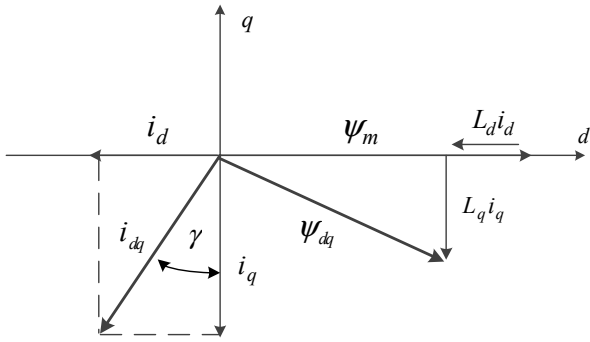


Fig. 3. Vector diagram of an IPMSG

Solution to that equation is the optimal current angle γ which ensures MTPA control:

$$\gamma = \arcsin \frac{-\psi_m + \sqrt{\psi_m^2 + 8I^2(L_q - L_d)^2}}{4(L_q - L_d)I} \quad (9)$$

Using (9) the optimal d -axis stator current can be expressed as a function of the q -axis stator current:

$$i_d = \frac{\psi_m}{2(L_q - L_d)} - \sqrt{\frac{\psi_m^2}{4(L_q - L_d)^2} + i_q^2} \quad (10)$$

For the desired electromagnetic torque, (3) and (10) are combined which results in quartic equation. Solution to that equation is the optimal d -axis stator current. After the optimal d -axis stator current is obtained, the optimal q -axis stator current is easily calculated using (3).

Optimal values of the d - and the q -axis stator currents calculated for different electromagnetic torque references form MTPA curve in dq plane. In Fig. 4 MTPA curve of the IPMSG used in simulation both considering and neglecting magnetic saturation is presented. While magnetic saturation can be neglected at lower stator current magnitudes, as the d - and the q -axis stator currents become larger magnetic saturation should be taken into account.

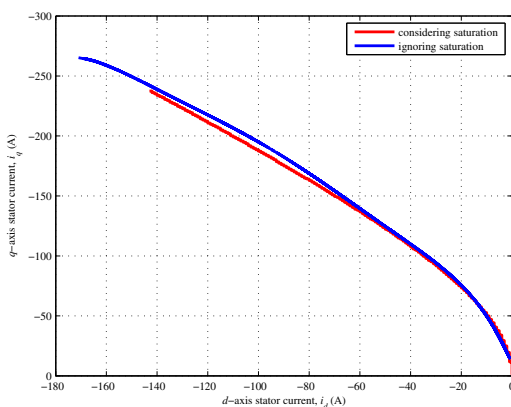


Fig. 4. MTPA curve considering and ignoring saturation

III. LOSS MINIMIZATION

The main power losses of an IPMSG are: copper loss, iron loss, stray loss and mechanical loss. The copper loss is the joule loss caused by stator coil resistance:

$$P_{Cu} = \frac{3}{2}(i_d^2 + i_q^2)R_s \quad (11)$$

The iron loss consists of hysteresis loss and eddy current loss and depends on frequency f and magnetic flux density B_m :

$$P_{Fe} = k_h f B_m^\alpha + k_e f^2 B_m^2 \quad (12)$$

where $k_h = 40-55$ is a constant which depends on the silicon contents in the steel, $k_e = 0.04-0.07$ is a constant which depends on the thickness of the steel lamination and silicon percentage, α is in the range 1.8-2.2, f is magnetic field frequency and B_m is maximum value of magnetic flux density [9]. The stray loss is caused by higher winding space harmonics and slot harmonics:

$$P_{str} = k_{str} \omega_e^2 (i_d^2 + i_q^2) \quad (13)$$

where k_{str} is the stray loss coefficient [15]. However, accurate calculation of the stray loss is difficult so its impact is neglected in this paper. The mechanical loss consists of friction and windage losses. It is proportional to the square of rotor speed:

$$P_{mech} = k_{mech} \omega_e^2 \quad (14)$$

where k_{mech} is the mechanical loss coefficient [18]. Since this loss does not directly depend on the stator current or the magnetic flux, it is uncontrollable.

In Fig. 5 equivalent circuit of an IPMSG is presented taking the iron loss into account. The iron loss is modelled as resistance which varies with angular electrical speed. The iron loss resistance can be measured by no load test when the stator current magnitude is only big enough to compensate the mechanical loss. In that case the iron loss is significant part of the input power.

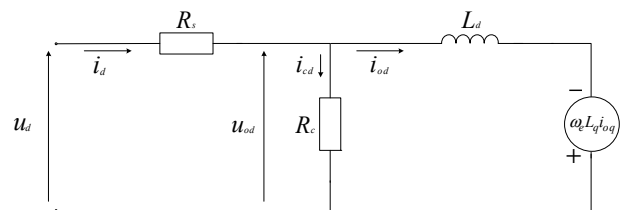


Fig. 5.a) d -axis equivalent circuit of an IPMSG

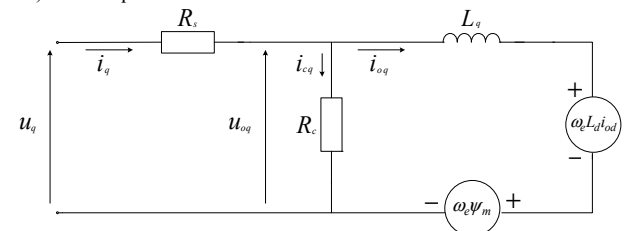


Fig. 5.b) q -axis equivalent circuit of an IPMSG

The mathematical model of an IPMSG in synchronously rotating dq reference frame considering the iron loss can be expressed as follows:

$$u_d = R_s i_{od} + L_d \frac{di_{od}}{dt} - \omega_e L_q \left(1 + \frac{R_s}{R_c} \right) i_{oq} \quad (15)$$

$$u_q = R_s i_{oq} + L_q \frac{di_{oq}}{dt} + \left(1 + \frac{R_s}{R_c} \right) (\omega_e L_d i_{od} + \omega_e \psi_m) \quad (16)$$

$$T_e = \frac{3}{2} p (\psi_m i_{oq} + (L_d - L_q) i_{od} i_{oq}) \quad (17)$$

where u_d and u_q are the d - and q -axis stator voltages, i_{od} and i_{oq} are the d - and the q -axis stator currents, ω_e is angular electrical speed, R_s is the stator resistance, R_c is the iron loss resistance, L_d and L_q are the d - and the q -axis inductances, ψ_m is the permanent magnet flux linkage, T_e is the electromagnetic torque and p is the number of pole pairs.

The iron loss resistance of the IPMSG used in simulation depending on rotor speed is shown in Fig. 6. Iron loss currents in the d - and the q -axis can be expressed as follows:

$$i_{cd} = - \frac{\omega_e L_q i_{oq}}{R_c} \quad (18)$$

$$i_{cq} = \frac{\omega_e (L_d i_{od} + \psi_m)}{R_c} \quad (19)$$

Total stator currents in the d - and the q -axis which cause the copper loss (11) can be expressed as follows:

$$i_d = i_{cd} + i_{od} \quad (20)$$

$$i_q = i_{cq} + i_{oq} \quad (21)$$

Using iron loss stator currents (18)-(19) and the iron loss resistance, the iron loss can be expressed as follows:

$$P_{Fe} = \frac{3}{2} (i_{cd}^2 + i_{cq}^2) R_c \quad (22)$$

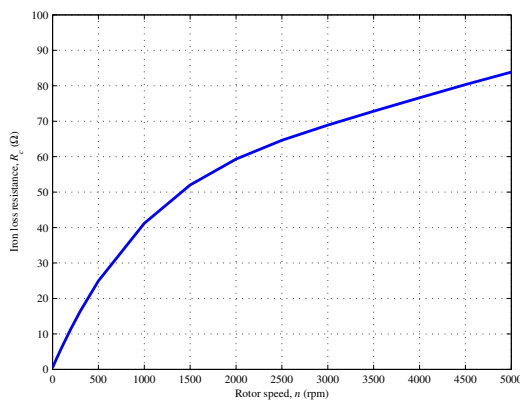


Fig. 6. Iron loss resistance depending on rotor speed

Neglecting the stray loss and the mechanical loss, total power loss of an IPMSG consists of the copper loss and the iron loss:

$$P_{loss} = P_{Cu} + P_{Fe} = \frac{3}{2} (i_d^2 + i_q^2) R_s + \frac{3}{2} (i_{cd}^2 + i_{cq}^2) R_c \quad (23)$$

The total power loss, the copper loss and the iron loss of the IPMSG used in simulation calculated for electromagnetic torque reference -400 Nm at rotor speed 2000 rpm are shown in Fig. 7. If (18)-(19) are used to substitute the d - and the q -axis iron loss currents in (23), the total power loss is expressed as a function of the d -axis stator current i_{od} , the q -axis stator current i_{oq} and angular electrical speed. For the desired electromagnetic torque, the q -axis stator current i_{oq} can be expressed as a function of the d -axis stator current i_{od} using (17). The total power loss now becomes only a function of the d -axis stator current i_{od} since the electromagnetic torque is known and angular electrical speed is calculated from measured rotor speed. In order to find the d -axis stator current which ensures the minimum total power loss, $\partial P_{loss} / \partial i_{od} = 0$ is calculated. After the optimal d -axis stator current is obtained, the optimal q -axis stator current is easily calculated using (17).

Optimal values of the d - and the q -axis stator currents calculated for different electromagnetic torque references at given rotor speed form LM curve in dq plane. In Fig. 8 LM curves of the IPMSG used in simulation for rotor speed values 500 rpm, 1300 rpm and 2000 rpm are presented.

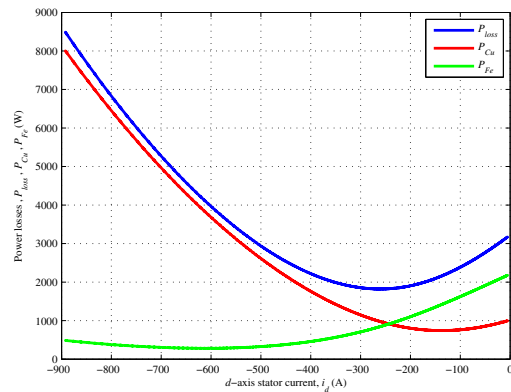


Fig. 7. Power losses depending on the d -axis current

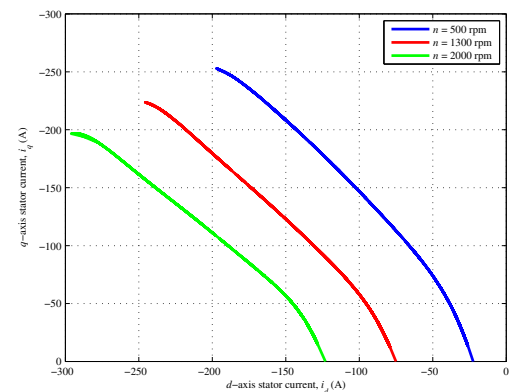


Fig. 8. LM curves for different rotor speed values

IV. SIMULATION RESULTS

Feed-forward torque control model was developed in MATLAB/Simulink to verify MTPA and LM control methods. Parameters of the IPMSG used in simulation are given in Table 1. For different electromagnetic torque references optimal stator currents considering magnetic saturation were calculated for both control methods and stored in lookup tables. Since LM takes into account the iron loss which depends on electrical angular frequency, calculations were made for different rotor speed values. For a given electromagnetic torque reference in the Simulink model, optimal stator currents were calculated using created lookup tables. Current control loop consists of the *d*- and the *q*-axis PI controllers and decoupling signals that ensure faster response. Parameters of PI controllers were calculated using technical optimum. Simulink model of the IPMSG was developed using the mathematical model considering the iron loss (15)-(21).

Described control methods were simulated. The electromagnetic torque reference was -400 Nm. The rotor speed was 2000 rpm initially and it dropped to 500 rpm at 0.05 s. The *d*- and the *q*-axis stator currents are shown in Fig. 9 and Fig. 10. The total power loss, the copper loss and the iron loss calculated for each operating point are presented in Table 2.

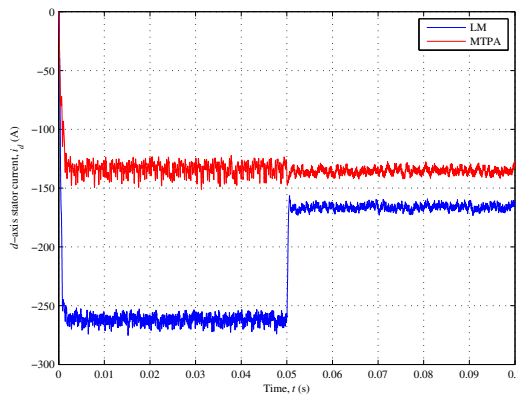


Fig. 9. *d*-axis stator current response

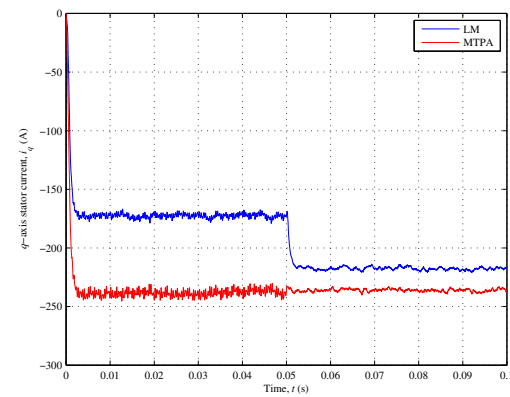


Fig. 10. *q*-axis stator current response

TABLE I. IPMSG PARAMETERS

| Parameter | Value |
|-------------------------------|------------------------------|
| Nominal voltage | $U_n = 355.9 \text{ V}$ |
| Nominal current | $I_n = 222.7 \text{ A}$ |
| Nominal power | $P_n = 118.5 \text{ kW}$ |
| Nominal torque | $T_n = 475.6 \text{ Nm}$ |
| Nominal rotor speed | $n_n = 2380 \text{ rpm}$ |
| Number of pole pairs | $p = 4$ |
| Stator resistance | $R_s = 6.67 \text{ m}\Omega$ |
| <i>d</i> -axis inductance | $L_d = 0.4905 \text{ mH}$ |
| <i>q</i> -axis inductance | $L_q = 1.3393 \text{ mH}$ |
| Permanent magnet flux linkage | $\psi_m = 0.213 \text{ Wb}$ |

At rotor speed 2000 rpm, the optimal *d*- and the *q*-axis stator currents for LM control method are -262 A and -171 A, respectively. The optimal *d*- and the *q*-axis stator currents for MTPA control method are -134 A and -236 A, respectively. Stator current magnitude is smaller in case of MTPA which results in smaller copper loss compared to LM. However, the iron loss is almost twice as big as the copper loss in case of MTPA which results in bigger total power loss compared to LM. Despite having bigger copper loss compared to MTPA, LM significantly reduces the iron loss with the negative *d*-axis stator current which results in smaller total power loss. The negative *d*-axis stator current produces magnetic flux in the opposite direction of the magnetic flux caused by permanent magnets which results in decrease of the *d*-axis magnetic flux. Since the iron loss depends on magnetic flux, decrease in magnetic flux causes smaller iron loss.

At rotor speed 500 rpm, the optimal *d*- and the *q*-axis stator currents for LM control method are -165 A and -217 A, respectively. The optimal *d*- and the *q*-axis stator currents for MTPA control method are -134 A and -236 A, respectively. Since MTPA solution does not depend on rotor speed and the electromagnetic torque reference has not changed, the optimal *d*- and the *q*-axis stator currents are the same for both simulated rotor speed values. The rotor speed value is four times smaller than in previous case which results in significantly smaller iron loss. Since the copper loss is much bigger than the iron loss at lower speed value, the optimal *d*- and the *q*-axis stator currents for LM and MTPA do not differ significantly.

TABLE II. CALCULATED POWER LOSSES

| Rotor speed | MTPA | LM |
|------------------------|-----------------------------|-----------------------------|
| $n = 2000 \text{ rpm}$ | $P_{Cu} = 738 \text{ W}$ | $P_{Cu} = 980 \text{ W}$ |
| | $P_{Fe} = 1417 \text{ W}$ | $P_{Fe} = 832 \text{ W}$ |
| | $P_{loss} = 2155 \text{ W}$ | $P_{loss} = 1812 \text{ W}$ |
| $n = 500 \text{ rpm}$ | $P_{Cu} = 731 \text{ W}$ | $P_{Cu} = 744 \text{ W}$ |
| | $P_{Fe} = 212 \text{ W}$ | $P_{Fe} = 188 \text{ W}$ |
| | $P_{loss} = 943 \text{ W}$ | $P_{loss} = 932 \text{ W}$ |

V. CONCLUSION

In this paper, MTPA and LM control methods were presented. For desired electromagnetic torque, MTPA control method finds the minimum stator current magnitude while LM control method finds the d - and the q -axis stator currents that ensure the minimum total power loss in IPMSG. Feed-forward torque control model in MATLAB/Simulink was used to verify described control methods. In order to achieve the minimum total power loss LM control method reduces the iron loss with negative d -axis stator current. On the other hand, MTPA control method does not take the iron loss into account which means it is independent of the rotor speed. Optimal stator currents according to MTPA depend only on the desired electromagnetic torque and IPMSG parameters. Since the iron loss depends on electrical angular speed, it becomes significant at high rotor speed values. MTPA control method finds optimal stator currents that minimize only the copper loss which results in significant difference between MTPA and LM optimal stator currents at high rotor speed values. At low rotor speed values the iron loss is significantly lower than the copper loss. Since the copper loss is dominant, MTPA and LM optimal stator currents do not differ significantly. Future work will be based on experimental validation of proposed control methods.

ACKNOWLEDGMENT

This work has been fully supported by the Croatian Science Foundation under the project number UIP-2013-11-7601.

REFERENCES

- [1] S. Brabic, N. Celanovic, and V. A. Katic, "Permanent magnet synchronous generator for wind turbine application," *IEEE Trans. Power Electron.*, vol. 13, no. 3, pp. 1136–1142, May 2008.
- [2] M. Chinchilla, S. Arnaltes, J.C. Burgos, "Control of permanent-magnet generators applied to variable-speed wind-energy systems connected to the grid," *IEEE Trans. on Energy Conversion*, vol. 21, no. 1, pp. 130-135, Mar. 2006
- [3] S. Morimoto, H. Nakayama, M.Sanada, Y. Takeda, "Sensorless output maximization control for variable-speed wind generation system using IPMSG," *IEEE Trans. Ind. Appl.*, vol. 41, no. 1, pp. 60-67, Jan./Feb. 2005.
- [4] W. Qiao, L. Qu, R.G. Harley, "Control of IPM synchronous generator for maximum wind power generation considering magnetic saturation," *IEEE Trans. Ind. Appl.*, vol. 45, no. 3, pp. 1095-1105, May/June 2009.
- [5] C.T. Pan and S.M. Sue, "A linear maximum torque per ampere control for IPMSM drives over full-load range speed," *IEEE Trans. Energy. Convers.* vol. 20, no. 2, pp. 359-366, June 2005.
- [6] S. Morimoto, Y. Takeda, and T. Hirasa, "Current phase control methods for permanent magnet synchronous motors," *IEEE Trans. Power Electron.*, vol. 5, no. 2, pp. 133-139, Apr. 1990.
- [7] S.Morimoto, M. Sanada, and Y. Takeda, "Wide-speed operation of interior permanent magnet synchronous motors with high-performance current regulator," *IEEE Trans. Ind. Appl.*, vol. 30, no. 4, pp. 920-926, Jul./Aug. 1994.
- [8] G. Kang, J. Lim, K. Nam, H.B. Ihm, H.-G. Kim, "A MTPA control scheme for an IPM synchronous motor considering magnet flux variation caused by temperature," *APEC 2004 nineteenth annual IEEE*, vol. 3, pp. 1617-1621, Feb. 2004.
- [9] S.Y. Jung, J. Hong, K. Nam, "Current minimizing torque control of the IPMSM using Ferrari's method," *IEEE Trans. Power Electron.*, vol 28., no. 12, pp. 5603-5617, Dec. 2013.
- [10] K.D. Hoang, J. Wang, M. Cyriacks, A. Melkonyan, K. Kriegel, "Feed-forward torque control of interior permanent magnet brushless AC drive for traction applications," Electric Machines & Drives Conference (IEMDC), 2013 *IEEE International*, pp. 152-159, May 2013.
- [11] T.M. Jahns, G.B. Kliman, T.W. Neumann, "Interior permanent-magnet synchronous motors for adjustable-speed drives," *IEEE Trans. Ind. Appl.*, vol. IA-22, no. 4, pp. 738-747, Jul./Aug. 1986.
- [12] S.Morimoto, Y.Tong, Y. Takeda, and T. Hirasa, "Loss minimization control of permanent magnet synchronous motor drives," *IEEE Trans. Ind. Electron.*, vol. 41, no. 5, pp. 511-517, Oct. 1994
- [13] S. Vaez, V.I. John, M.A.Rahman, "An on-line loss minimization controller for interior permanent magnet motor drives," *IEEE Trans. on Energy Conversion*, vol. 14, no. 4, pp. 1435-1440, Dec.1999.
- [14] C.Cavallaro, A.O.D. Tommaso, R.Miceli, A. Raciti, G.R. Galluzzo, and M.Tranpanese, "Efficiency enhancement of permanent-magnet synchronous motor drives by online loss minimization approaches," *IEEE Trans. Ind. Electron.*, vol. 52, no. 4, pp.1153-1160, Aug. 2005
- [15] J. G. Lee, K. H. Nam, S. H. Lee, S. H. Choi, and S. W.Kwon, "A lookup table based loss minimizing control for FCEV permanent magnet synchronous motors," *Journal of Electrical Engineering & Technology*, vol. 4., no. 2, pp. 201-210, Jun. 2009.
- [16] J. Lee, K. Nam, S. Choi, S. Kwon, "Loss Minimizing Control of PMSM with the Use of Polynomial Approximations," *Industry Applications Society Annual Meeting, 2008. IAS '08. IEEE*, pp. 1-9, Oct. 2008.
- [17] C. Mademlis, V.G. Agelidis, "On considering magnetic saturation with maximum torque to current control in interior permanent magnet synchronous motor drives," *IEEE Trans. Energy. Convers.*, vol. 16, no. 3, pp. 246-252, Sept. 2001.
- [18] C. Mademlis, I. Kioskeridis, N. Margaris, "Optimal efficiency control strategy for interior permanent-magnet synchronous motor drives," *IEEE Trans. Energy. Convers.*, vol. 19, no. 4, pp. 715-723, Dec. 2004